

Discovery of ammonoid jaw apparatus and associated features using reflectance transformation imaging (RTI)

DANIEL ANDRÉS MORÓN-ALFONSO¹
MARCELA CICHOWOLSKI¹

RENÉ HOFFMANN²
MARICEL GABRIELA RODRIGUEZ³

1. Instituto de Estudios Andinos "Don Pablo Groeber", Consejo Nacional de Investigaciones Científicas y Técnicas (IDEAN- CONICET). Intendente Guiraldes 2160, Ciudad Universitaria, Pabellón 2, Piso 1, C1428EGA Ciudad Autónoma de Buenos Aires, Argentina.
2. Institute of Geology, Mineralogy, & Geophysics, Ruhr-Universität Bochum, C44721. Universitätsstraße 150, 44801 Bochum, Germany.
3. Instituto de Química, Física de los Materiales, Medio Ambiente y Energía, Consejo Nacional de Investigaciones Científicas y Técnicas (INQUIMAE-CONICET), Departamento de Química Inorgánica, Analítica y Química Física, Facultad de Ciencias Exactas y Naturales, Universidad de Buenos Aires. Intendente Guiraldes 2160, Pabellón 2, Piso 3, Ciudad Universitaria, C1428EGA Ciudad Autónoma de Buenos Aires, Argentina.

Recibido: 9 de junio 2022 - Aceptado: 28 de diciembre 2022 - Publicado: 1 de marzo 2023

Para citar este artículo: Daniel Andrés Morón-Alfonso, Marcela Cichowolski, René Hoffmann, & Maricel Gabriela Rodríguez (2023). Discovery of ammonoid jaw apparatus and associated features using reflectance transformation imaging (RTI). *Publicación Electrónica de la Asociación Paleontológica Argentina* 23 (1): 34–48.

Link a este artículo: <http://dx.doi.org/10.5710/PEAPA.28.12.2022.430>

©2023 Morón-Alfonso, Cichowolski, Hoffmann, & Rodríguez



This work is licensed under

CC BY-NC 4.0



ISSN 2469-0228

Asociación Paleontológica Argentina
Maipú 645 1° piso, C1006ACG, Buenos Aires
República Argentina
Tel/Fax (54-11) 4326-7563
Web: www.apaleontologica.org.ar

DISCOVERY OF AMMONOID JAW APPARATUS AND ASSOCIATED FEATURES USING REFLECTANCE TRANSFORMATION IMAGING (RTI)

DANIEL ANDRÉS MORÓN-ALFONSO¹, MARCELA CICHOWOLSKI¹, RENÉ HOFFMANN², AND MARICEL GABRIELA RODRIGUEZ³

¹Instituto de Estudios Andinos "Don Pablo Groeber", Consejo Nacional de Investigaciones Científicas y Técnicas (IDEAN- CONICET). Intendente Guiraldes 2160, Ciudad Universitaria, Pabellón 2, Piso 1, C1428EGA Ciudad Autónoma de Buenos Aires, Argentina. paleokarzis@gmail.com; mcicho@gl.fcen.uba.ar

²Institute of Geology, Mineralogy, & Geophysics, Ruhr-Universität Bochum, C44721. Universitätsstraße 150, 44801 Bochum, Germany. Rene.hoffmann@rub.de

³Instituto de Química, Física de los Materiales, Medio Ambiente y Energía, Consejo Nacional de Investigaciones Científicas y Técnicas (INQUIMAE-CONICET), Departamento de Química Inorgánica, Analítica y Química Física, Facultad de Ciencias Exactas y Naturales, Universidad de Buenos Aires. Intendente Guiraldes 2160, Pabellón 2, Piso 3, Ciudad Universitaria, C1428EGA Ciudad Autónoma de Buenos Aires, Argentina. mgrodriguez@qi.fcen.uba.ar

ORCID DAMA: <https://orcid.org/0000-0002-8865-8370>; MC: <https://orcid.org/0000-0002-9079-6350>; RH: <https://orcid.org/0000-0001-7992-1264>; MGR: <https://orcid.org/0000-0003-0809-8631>

Abstract. We report on remains of the buccal apparatus and possible associated structures for the Late Cretaceous ammonite *Maorites seymourianus* from the López de Bertodano Formation (Antarctic Peninsula). This is the first description of these structures for the family Kossmaticeratidae. Further, we discuss the most likely taphonomic processes taking place that allowed this exceptional preservation. Reflectance Transformation Imaging (RTI) technique was employed in this work to better document the faint structures. We briefly provide a review of this method and its potential importance for paleontological studies because it seems that this powerful technique has been largely overlooked by paleontologists.

Key words. Ammonoid. Jaw Apparatus. RTI. Kossmaticeratidae. *Maorites seymourianus*. Antarctica.

Resumen. DESCUBRIMIENTO DE MANDÍBULAS DE AMONITES Y POSIBLES ESTRUCTURAS ASOCIADAS USANDO REFLECTANCE TRANSFORMATION IMAGING (RTI). En este trabajo se reporta la presencia de elementos del aparato bucal y posibles estructuras asociadas en un amonite de la especie *Maorites seymourianus* de la Formación López de Bertodano (Cretácico Tardío, Península Antártica), y se discuten los procesos tafonómicos que habrían permitido esta preservación excepcional. Esta es la primera descripción de estas estructuras para la familia Kossmaticeratidae. Para este estudio se empleó una técnica denominada *Reflectance Transformation Imaging* (RTI) relativamente poco aplicada en estudios paleontológicos, por lo que se provee una breve revisión del método y se indica su potencial importancia para estos estudios.

Palabras Clave. Ammonoida. Aparato Bucal. RTI. Kossmaticeratidae. *Maorites seymourianus*. Antártida.

THE LAST decade has shown several technological breakthroughs that have led to original discoveries in paleontology and related sciences, particularly by the use of new imaging, isotopic, and virtual techniques, driven by the increase in resolution and processing computational power (Cunningham *et al.*, 2014; Giovannetti *et al.*, 2016; Sutton *et al.*, 2016; Pan *et al.*, 2019; Pérez-Ramos & Figueirido, 2020). Specifically for extinct cephalopods like the ammonoids, this kind of technical innovations have been key to the description of structures which would have been rarely found in this group otherwise. Examples include the employment of a wide variety of tomographic techniques such as grinding tomography, X-ray microtomography, synchrotron tomography, and

neutron tomography (*e.g.*, Hoffmann *et al.*, 2013; Tajika *et al.*, 2015; Takeda *et al.*, 2016; Kruta *et al.*, 2020; Cherns *et al.*, 2021; Smith *et al.*, 2021; Tanabe *et al.*, 2021), laser-induced fluorescence (Barlow *et al.*, 2021), and digitization techniques such as surface or 3D scanning and photogrammetry (Peterman *et al.*, 2019, 2020). Ammonoids are extinct cephalopods that appeared during the Early Devonian and went extinct at the Cretaceous/Paleogene boundary, with a few members eventually surviving into the earliest Paleogene (Landman *et al.*, 2015). These organisms shared an external aragonitic shell similar to the modern *Nautilus* Linnaeus, 1758, but are phylogenetically closer to coleoids (Kröger *et al.*, 2011; Klug *et al.*, 2015). The ammonoid shell is divided

internally by the phragmocone and the body chamber. The former is subdivided in itself by usually complex septa that limit chambers (likely filled with gas or a low-density fluid; Klug & Hoffmann, 2015), which are connected through a generally ventral organic tube known as the siphuncle (Tanabe *et al.*, 2015b). This tube connects all chambers of the phragmocone, including its initial chamber, and reaches the body chamber that allocates most of the soft parts of the organism including all the organs and muscular tissues (Klug & Lehmann, 2015). As follows, the phragmocone was the principal buoyancy device of the organism and the body chamber contained and protected the soft parts of the body.

Reflectance Transformation Imaging (RTI; Schroer, 2012) is a technique based on the fundamental principles of Polynomial Texture Mapping (PTM; Hammer *et al.*, 2002). It is widely used in computer-generated imagery (CGI), and has been successfully applied to document minute surface features (<1 μm) principally in archeological objects of cultural and heritage value (e.g., Palma *et al.*, 2010; Boute *et al.*, 2018; Morita *et al.*, 2019; Min *et al.*, 2021). In contrast to the power of the method to depict minute surface details useful for fossil identification, RTI has been rarely applied to study fossil material (e.g., Van Bocxlaer & Schultheiß, 2010; Hammer & Spocova, 2013; Klug *et al.*, 2019; Guo *et al.*, 2022). That comes as a surprise, but it is likely because the original technique, PTM, required complex hardware, im-

practical to adapt to different fossil samples (e.g., Hammer *et al.*, 2002; Béthoux *et al.*, 2016; Klug *et al.*, 2019). This limitation has been overcome with a more advanced RTI technique, allowing its implementation in variable conditions (Schroer, 2012). Here, we apply RTI to report for the first time organic remains found within the body chamber of an exceptionally well-preserved Maastrichtian *Maorites seymourianus* (Kilian & Reboul, 1909). Findings include elements of the jaw apparatus and structures that are potentially related to the buccal mass but difficult to identify. Further, we provide a summary of the RTI technique and discuss the possible advantages of the method.

MATERIAL AND METHODS

The herein-described *Maorites seymourianus* specimen (Fig. 1) was collected *ex-situ* by Dr Andrea Concheyro during the summer Antarctic campaign of 1990 and 1991, from the upper deposits ("Molluscan units") of the López de Bertodano Formation that outcrop in the Vicecomodoro Marambio Island (Seymour Island in English literature), Antarctic Peninsula (Macellari, 1986, 1988). The Molluscan units (Units 7 to 9, Macellari, 1988; Montes *et al.*, 2019) are a thick sequence of generally monotonous sandy siltstone that contains a rich and very abundant molluscan fauna. The dominant lithology is a dark, friable, bioturbated silty sandstone with minor intercalations of fine-grained glauconitic sandstone.

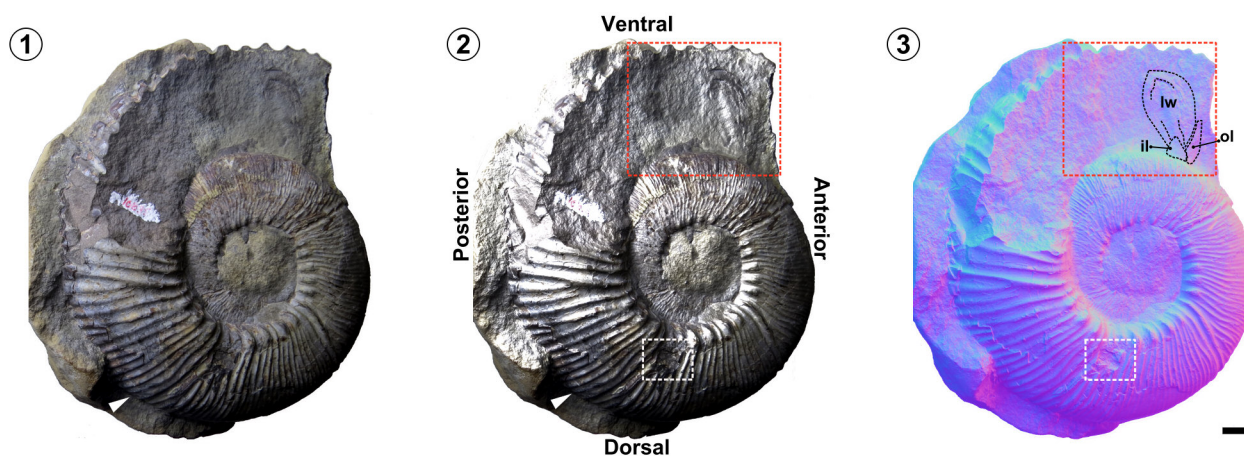


Figure 1. *Maorites seymourianus*, CPBA-16835 in lateral view. **1**, default view; **2**, specular enhanced view (Supplementary material 1, RTI file A, light coordinates: $X = -0.20$, $Y = 0.53$, parameters: $dc = 72$, $sp = 72$, $hs = 80$). The red square indicates the region of interest where the features were found. The white one is the location of the pathology. The white arrow indicates the end of the phragmocone; **3**, normal map of the specimen showing the position of jaw elements as black dotted lines. Scale bar = 10 mm.

It is inferred to have been deposited in middle-shelf to shelf-slope break environments (Macellari, 1988; Olivero, 2012).

According to the age model proposed by Tobin *et al.* (2012) and Witts *et al.* (2015), *M. seymourianus* is recorded in the late Maastrichtian, ranging from 69 Ma to 68.3 Ma, and would have inhabited a shallow marine to transitional environment (Macellari, 1988; Olivero, 2012; Morón-Alfonso, 2019; Scasso *et al.*, 2020). The specimen is housed at the Colección Paleontológica de Buenos Aires (CPBA) of the Facultad de Ciencias Exactas y Naturales, Universidad de Buenos Aires (Argentina), under the number CPBA-16835. This specimen is a three-dimensionally preserved conch with a maximum diameter of 147 mm consisting of a complete phragmocone and body chamber. The body chamber is naturally fractured following an approximate longitudinal section where the structures were found. Most of the original aragonitic shell material is preserved but partially embedded in a carbonate concretion with dimensions of 156 x 61 x 135 mm; the counterpart of this concretion is missing (Fig. 1).

Reflectance Transformation Imaging

Reflectance Transformation Imaging is a computational photographic technique used in the examination of surfaces providing enhanced visualization of their color and/or relief using multi-lighting conditions (Hammer & Spocova, 2013). RTI files are generated from a set of images captured with the camera in a fixed position. In the next step, the software calculates a normal map based on the incident angles in which the light bounces from the studied surface (Fig. 1.3). In this work, we used the procedure described by Schroer (2012) in which black spheres replace the light dome used in previous applications of this method (Hammer & Spocova, 2013). Detailed guides and tutorials can be found at <http://culturalheritageimaging.org/>. The CPBA-16835 specimen was placed onto a non-reflective surface under different lighting orientations and potential output (1W and 3W, respectively). We used the open-source software RTIBuilder 2.0.2 and RTIviewer 1.0.1 for image processing and visualization (Boute *et al.*, 2018). Four RTI files were generated for this study, two of the complete specimen and two of the body chamber. Each RTI file was composed of around 50 images (some were manually removed due to errors). Additionally, complementary photos with a higher resolution

were taken emulating the light coordinates based on the RTI files. Focus stacking and image stitching were also used to generate detailed images and 3D models of smaller features using Helicon Focus 8.0.4 (Kozub *et al.*, 2022) and the Image Composite Editor 2.0.3.0 (Microsoft-Corporation, 2015), respectively. Lastly, virtual models of the lower and upper jaw were generated using Blender 3.1.2 (Blender Online Community, 2022) to test different possible jaw movements. The models were generated based on the normal maps obtained from the RTI files. Normal maps are images that store the direction at each pixel in a RGB color model. These normal maps were translated into surfaces, and then digitally sculpted into models.

X-Ray Diffraction (XRD), Scanning Electron Microscope (SEM), and Energy Dispersive Spectroscopy (EDS) Analyses

Four regions from the body chamber's specimen were analyzed using a Panalytical Empyrean Powder Diffractometer located in the INQUIMAE (Instituto de Química, Física de Materiales, Medio Ambiente y Energía, Universidad de Buenos Aires) facility. For this, it was employed a Cu radiation of $K_{\alpha 1} = 1.54 \text{ \AA}$ and the device was equipped with a PIXcel3D area detector in the range of 10–120 degrees in a *theta/2 theta* configuration. The step was set up to 0.026 degrees and the count time to 200 seconds. The device was calibrated with a Silicon standard with a detection limit ranging from 0.5–2%. For the resulting diffractograms, a search was performed using the COD (Crystallography Open Database) database in the HighScorePlus V5.1 (Degen *et al.*, 2014) to identify the elemental composition of the selected area.

Additionally, to screen for diagenetic alteration, two shell fragments of the studied specimen were examined under SEM Philips 505 located at the Instituto Nacional de Tecnología Industrial (INTI, Argentina) with an acceleration voltage of 15 kV, and a probe current of 36–54 pA. The working distance was approximately 10 mm. Further, their chemical composition was identified using an energy-dispersive X-ray spectroscopy system attached to the SEM in combination with EDAX analytical software.

Anatomical abbreviations. **ap**, aptychus; **c**, crest; **ct**, calcified tip; **dt**, denticle; **gv**, groove; **il**, inner lamella; **ma**, muscular attachment site; **lo**, lanceolate object; **lw**, lateral wall; **ol**,

outer lamella; r, rostrum; t_n , trace n.

Other abbreviations. CGI, computer-generated imagery; dc, diffuse color; ds, dark/dim surface; EDS, Energy Dispersive Spectroscopy; hs, highlight size; ms, mineral surface layer; pr, positive relief; PTM, polynomial texture mapping; RTI, reflectance transformation imaging; SEM, scanning electron microscope; sp, specularity; XRD, X-ray diffraction.

RESULTS

The resulting RTI files and additional images can be found in Supplementary material 1 and visualized using the RTIviewer 1.0.1 software. To replicate the images in this paper, we also provide the light position (x and y coordinates) and the values for the specular enhancement view: dc, sp, and hs. We encourage the reader to vary these parameters as several of the structures described below are highlighted under different lighting conditions.

Structures observed within the body chamber of *Maorites seymourianus* (CPBA-16835) are interpreted as remnants of the buccal mass, and most of them are preserved as imprints, barely visible to the naked eye (Figs. 1–2). Jaw elements are identified and will be described in detail below. All other features poorly preserved will be tentatively interpreted using the nomenclature provided by Tanabe *et al.* (2015a).

Lower jaw

The most noticeable structure observed is a flattened cast of the left lateral side of an ap of the lower jaw (Figs. 2–4). The structure would have been lying upside down, providing an internal view showing a possible c, the lw, and the r (Figs. 2–4). XRD analysis reveals that most of this structure (a1 in Fig. 2) was diagenetically altered to amorphous silica and silicate minerals, it seems that only the ct of the r kept its original composition. The flattened cast of the elongated pear-shaped ap is around 25 x 13 mm in size. It is slightly tilted adorally with its narrow section pointing forward (Fig. 3). The anterior region of this lower jaw is delimited by an irregular thickening marking a possible c with a couple of sharp indentations, possibly signalling the presence of dt (Figs. 3, 5; Tanabe *et al.*, 2015a: fig. 10.4). The c extends in an arc towards the anterodorsal region turning into a sharp subtriangular depression marking the r and ending up in a sharp tip (Figs. 3, 5). The ventral posterior section of the lw shows an irregular topography and is apparently attached to a soft pr discussed below (Figs. 3–4). The anterodorsal area of the lower jaw is well-defined by an almost straight furrow, interpreted here as a possible muscle attachment site (Figs. 3–4). This furrow disappears under the il of the upper jaw. Depending on the lighting conditions, growth lines can be observed in the cast of the lw (Fig. 3.1–2).

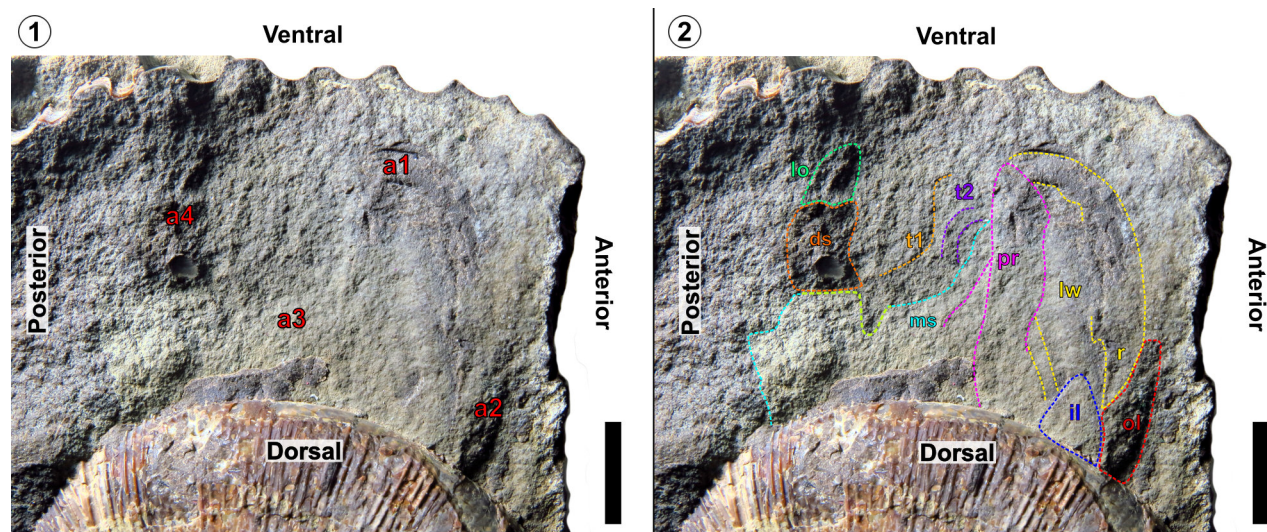


Figure 2. Body chamber indicating the spatial distribution of the structures found in *Maorites seymourianus*, CPBA-16835. 1, body chamber showing the four areas studied using x-ray diffraction (XRD) analysis; 2, highlight of the structures observed on the body chamber. Scale bar= 10 mm.

Upper jaw

XRD analysis (a2 in Fig. 2) found on the studied specimen indicates the presence of calcite, showing that despite being less evident than the elements of the lower jaw, its original carbonatic composition remains. Parts of the upper jaw can only be observed using particular RTI parameters and light orientations (indicated in Figs. 3–4). The first component is a cast of the subtriangular *il* with a soft ridge in the posterior margin (Figs. 3–4). This structure is about 10 x 7 mm in size and seems to be overlapped (indicated by a *gv*) by the darker beak-shaped *ol* (Fig. 5). The latter is 15 x 7 mm in size and seems to overlay the *r* of the lower jaw. The tip of the *ol* seems blunt, but this could be just an effect of the slight decoloration of the surrounding area (Fig. 5). It is unclear if these components correspond to both paired

elements deformed and flattened, or if it is just one of these elements in lateral view.

Additional structures

Several enigmatic structures were observed in the studied specimen. One of them is a smooth *pr* around the anterior region of the body chamber and seems to be connected to the posterior margin of the *lw* in the lower jaw (Figs. 2–4). This structure is around 26 x 7.5 mm in size (Figs. 2–4). It is irregular in shape and shows a deep prolongation towards the *c* (Fig. 3). Contrary, the posterior margin of this *pr* is uniform and follows an almost straight line towards the dorsum of the whorl, fainting behind the *ma* in the lower jaw. This elevated surface has a smooth outlook, showing several minor linear depressions, and a couple of deep crevasses (Fig. 3).

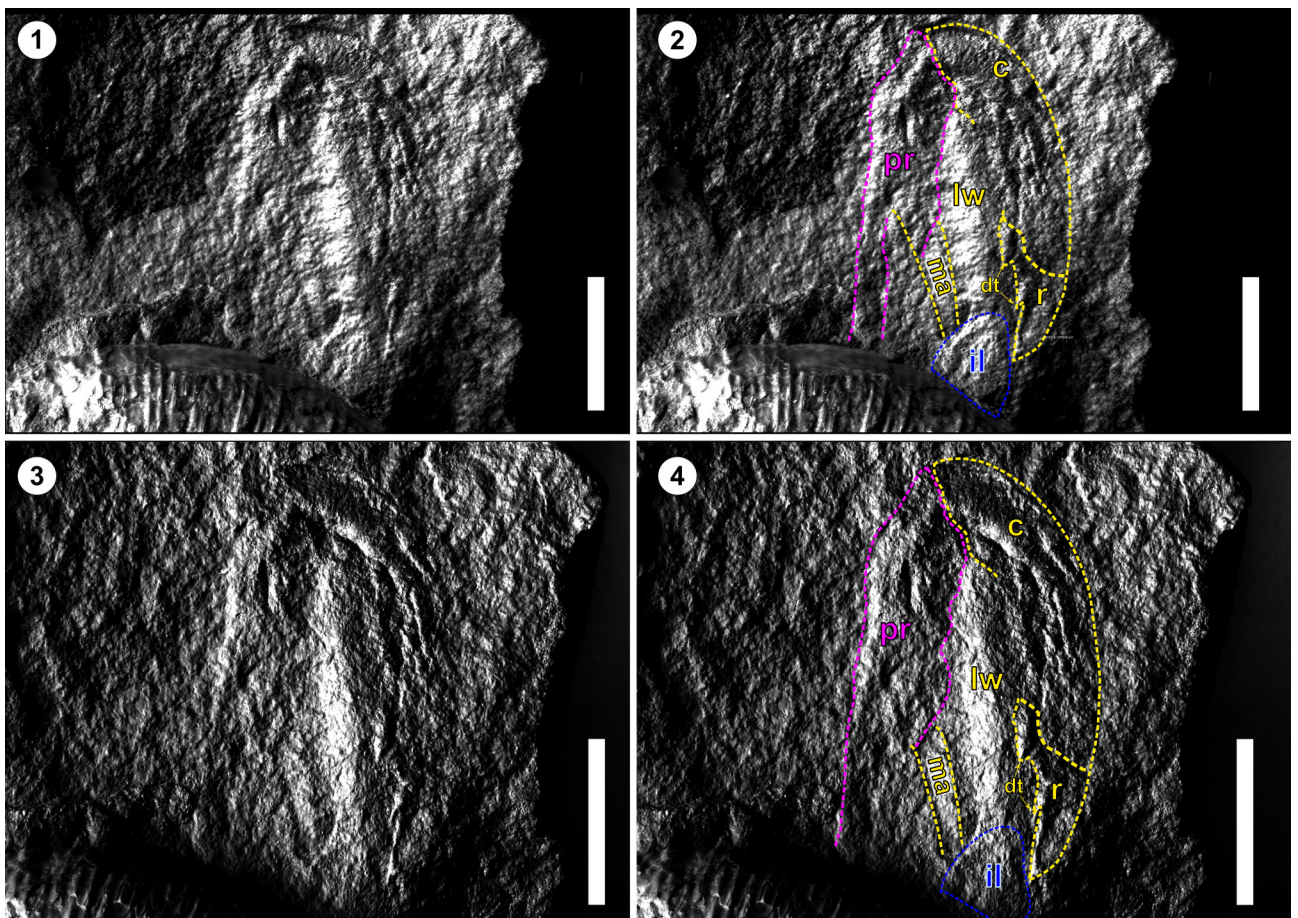


Figure 3. Specular enhanced images of the lower jaw in RTI files of the body chamber of *Maorites seymourianus*, CPBA-16835. 1–2, highlight of the lower jaw components showing the growth lines (Supplementary material 1, RTI file B, light coordinates: X = -0.33, Y = 0.69, parameters: dc = 37, sp = 70, hs = 75); 3–4, different orientation of the specimen underlining the denticles and the sharp tip of the rostrum (Supplementary material 1, RTI file C, light coordinates: X = 0.99, Y = 0.11, parameters: dc = 1, sp = 93, hs = 64). Scale bar = 10 mm.

At the posterior margin of the pr, a relatively thick layer of a white mineral is present (ms; Fig. 4; Supplementary material 2). XRD analysis of this surface (a3 in Fig. 2) indicates that it is likely composed of periclase associated with ferropiclase, magnesiowüstite, and fluorite. This feature is characterized by a smoother texture compared to the surrounding matrix (Fig. 4; Supplementary material 2). The ventral area of this surface is well-defined near the

buccal mass and towards its distal area, but it is interrupted by an engulfed section and a ds around its center (Fig. 4, 6).

The ds is 14 x 19 mm in size. It corresponds to the second enigmatic structure present in the specimen, which also connects to a lo (preserved as a cast) at the bottom (Fig. 6). When the effect of the color is removed (using dc), both structures (ds, lo) are accentuated revealing noticeable textural variations. In these conditions, the ds shows small

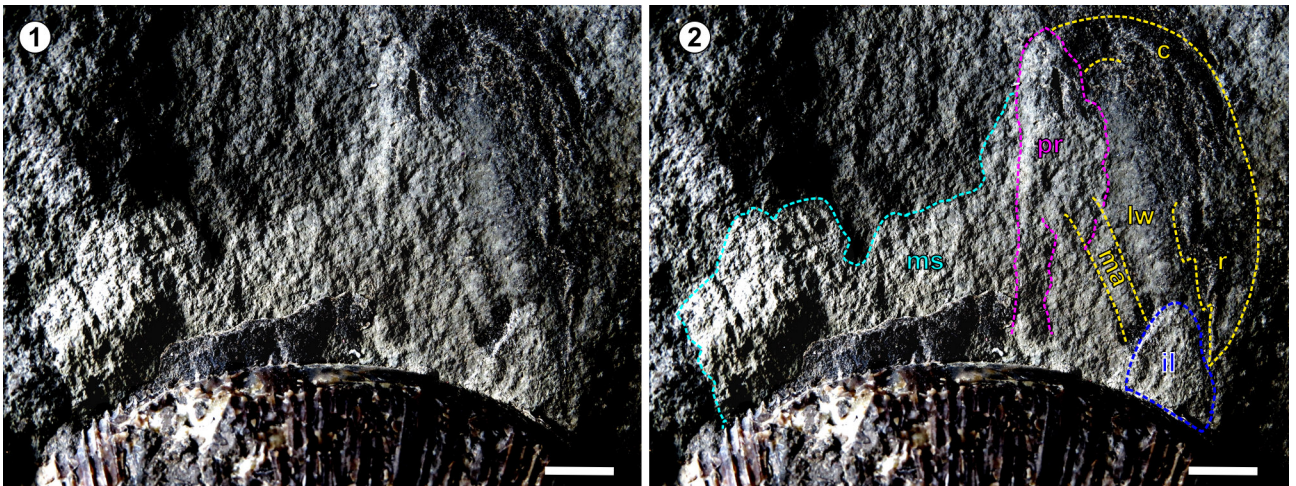


Figure 4. Composite image of the region of interest highlighting the mineral surface and the buccal apparatus components of *Maorites seymourianus*, CPBA-16835. 1, clean view of the structures observed on the specimen; 2, highlight of the structures observed with respective labels (Image based on Supplementary material 1, RTI file B, light coordinates: X = 0.46, Y = 0.51, parameters: dc = 0, sp = 69, hs = 43). Scale bar= 5 mm.

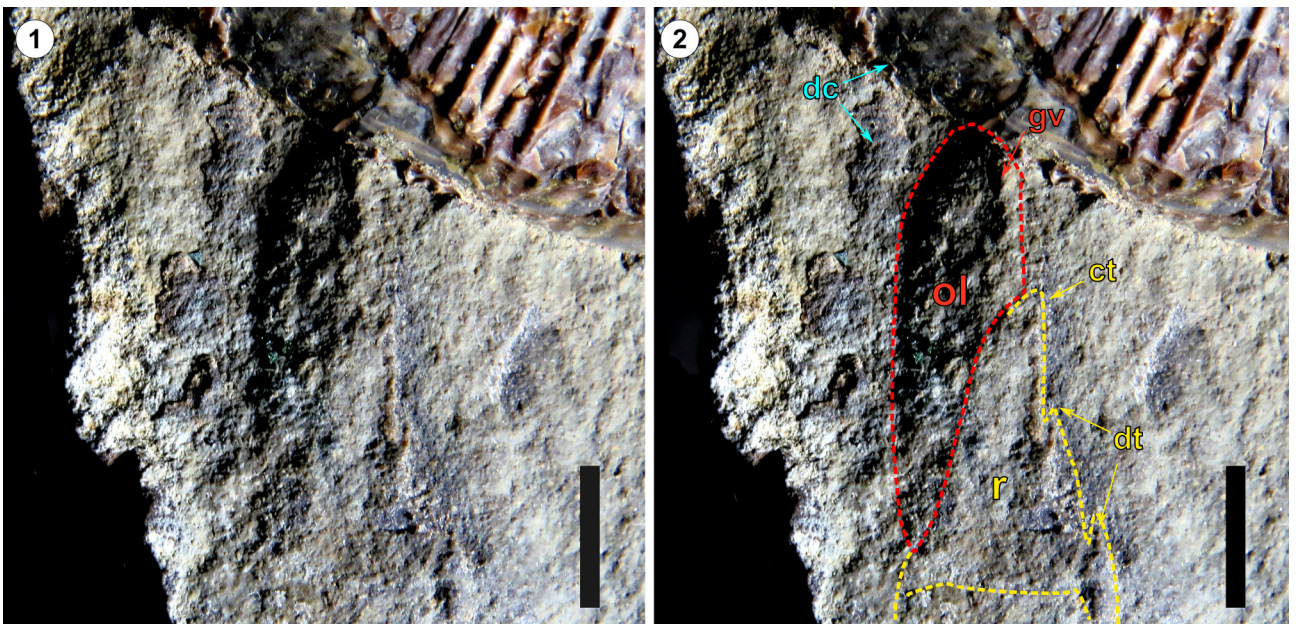


Figure 5. Close-up of the ol in life position, showing the elements of the rostrum of *Maorites seymourianus*, CPBA-16835. 1, clean view of the structures observed in this region; 2, highlight of the structures with respective labels. Scale bar= 5 mm.

traces observed as bright irregular marks, and a prominent translucent fragment around its center (Figs. 6–8). This convex fragment is 3.2 x 3.8 mm in size and has an irregular

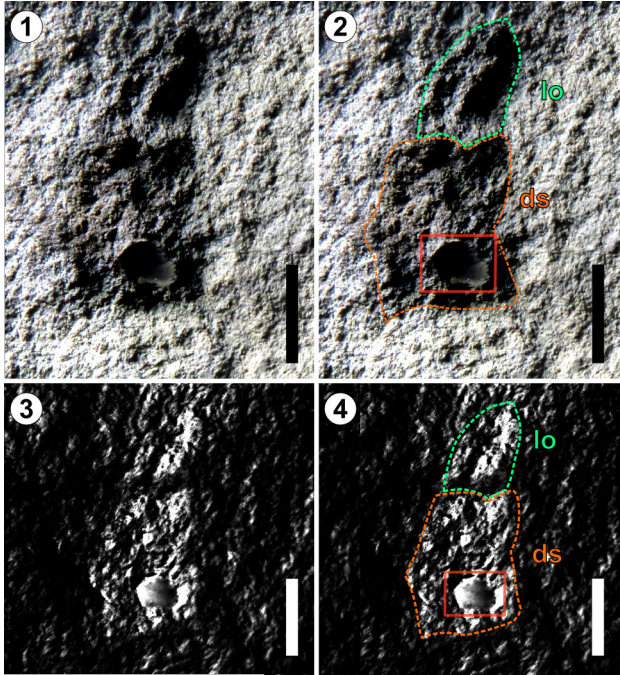


Figure 6. *Maorites seymourianus*, CPBA-16835. 1–2, detail of ds and lo indicated in Figure 2. The red square marks the position of the organic fragment; 3–4, specular enhanced image with color completely diffused, only textural levels are highlighted. Note that both features are accentuated with respect to the surrounding matrix, and the traces in the dim area (Supplementary material 1, RTI file C, light coordinates: X = 0.70, Y = -0.71, parameters: dc = 0, sp = 92, hs = 93). Scale bar = 10 mm.

outline (Fig. 7.1). It also has an oval white mark, and when illuminated with low light, concentric lines can be observed on its surface (Fig. 7.2). Further, the lo located just under ds is 12.8 x 9.8 mm in size and is separated from the contiguous feature by a gv (Fig. 6; Supplementary material 2). The lo has a ridge in its center that curves anteriorly and flattens laterally. XRD analysis of the ds (a4 in Fig. 2) showed that this region has a complex composition, signalling the possible presence of manganese, silica, molybdenum, nickel, hydrogen, carbon, and phosphorus. However, due to the irregular concave topography of this surface in the body chamber, there is considerable noise present on the diffractograms, so results are unreliable. Due to this difficult topography, we were unable to identify the composition of the translucent fragment as well.

Adjacent to the ds there are a few additional delicate traces named here as t_1 and t_2 (Fig. 8.2). The former is around 17 mm in length and seems to form an arc towards the ventral region. The latter is 12 mm at its maximum length, and it appears to be a pair of concentric lines nearby the lower jaw (Fig. 8). Lastly, around the middle of the whorl and located near the end of the phragmocone, there is a 9.8 mm long and 6 mm wide ellipsoidal perforation in the shell wall partially filled partially with sediment (pointed with white arrows in Fig. 9.1–9.2).

SEM and EDAX results showed that the shell preserved its original structure and composition, conserving the pris-

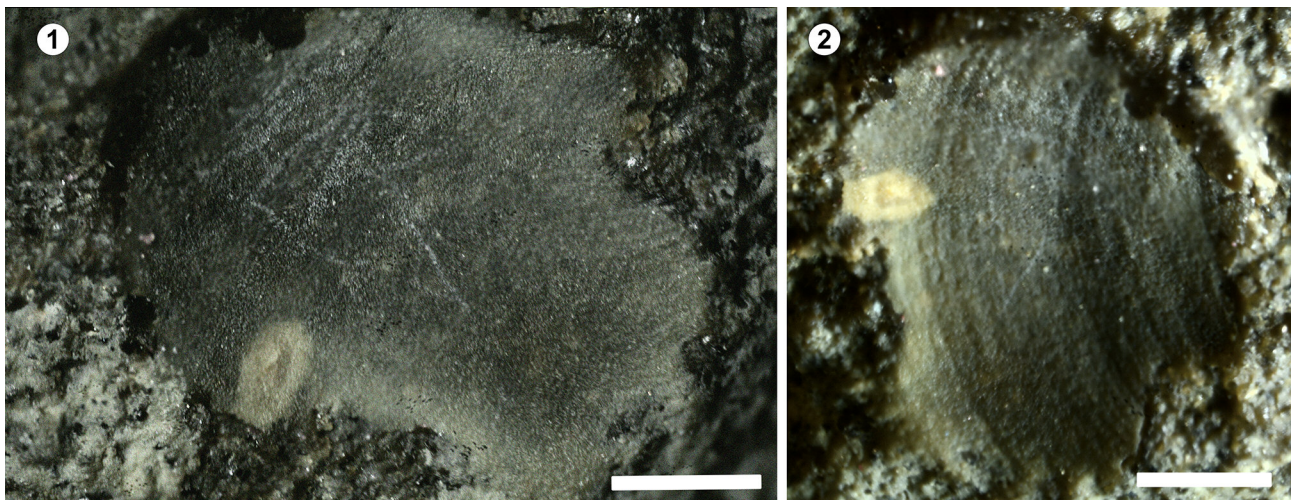


Figure 7. *Maorites seymourianus*, CPBA-16835, detail of the concave organic translucent fragment using different light conditions. 1, the translucent fragment under direct light. Note that the matrix can be seen through the material; 2, the same translucent fragment with a different orientation and under a tangent light showing the concentric lines. Scale bar = 1 mm.

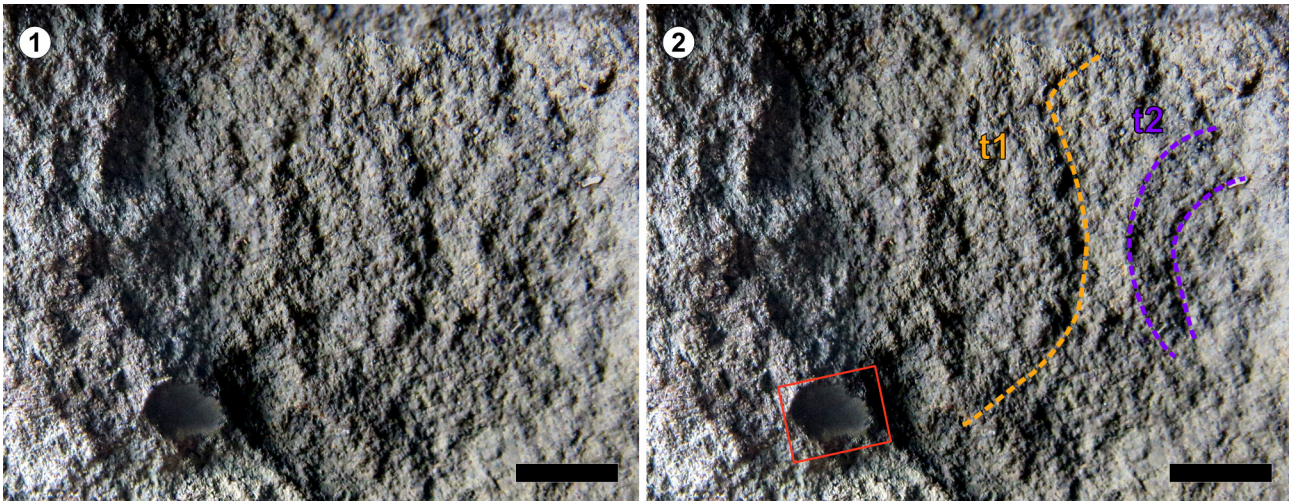


Figure 8. *Maorites seymourianus*, CPBA-16835. Faint traces found in the body chamber of the specimen. 1, clean view of the region of interest; 2, highlight of the traces observed. The red square indicates the location of the organic fragment for orientation. Scale bar = 10 mm.



Figure 9. Highlight of the phragmocone of *Maorites seymourianus*, CPBA-16835, showing the elliptical mark interpreted as a pathology (red arrow). 1, default view; 2, specular enhanced view. Scale bar = 5 mm. (Supplementary material 1, RTI file B, light coordinates: X = -0.47, Y = 0.10, parameters: dc = 32, sp = 43, hs = 139).

matic and nacreous layers (Fig. 10, Supplementary material 2). Therefore, diagenetic alteration of the shell is not recognized in the studied specimen.

DISCUSSION

Here, we provide the first report of a jaw apparatus for Kossmaticeratidae. Moreover, our finding represents the youngest occurrence of ammonoid jaws based on current age models (Tanabe *et al.*, 2015a; Witts *et al.*, 2015). This observation implies that most of the structures conforming the jaw apparatus previously reported for ammonoids (Tanabe *et al.*, 2015a) persisted into the late Maastrichtian without

significant morphological changes (Witts *et al.*, 2015). Due to the lack of hard parts of the jaw elements, it is difficult to assign the herein-described jaw apparatus to a specific type following the classification presented in Tanabe *et al.* (2015a). Previous reports for Desmoceratoidea suggest that the lower jaws are weakly calcified and principally composed of chitinous elements (Tanabe *et al.*, 2015a). Circumstantial support for the poorly calcified jaw structures comes from the fact that they have not been reported before, even as isolated fossils, which comes as a surprise considering the high abundance of ammonites reported for the López de Bertodano Formation (Macellari, 1986; Witts *et*

al., 2015). Given the presence of transitional features from the anptychus-type to the aptychus-type, and the variable mineralogy and microstructure of the jaw components, Tanabe *et al.* (2015a) determined an “Intermediate Type” for the desmoceratoid jaw apparatuses so *Maorites seymourianus* (CPBA-16835) may belong to this category as well. The lower jaw found in the studied specimen also resembles the recently reported jaws for boreal Valanginian ammonites of the family Polyptychitidae (Mironenko & Mitta, 2023), specifically in the acute apical angle and the sharp rostra rarely found in Cretaceous ammonites. The upper jaw also exhibits specific characteristics showing an ol with a slender profile, and a relatively small il. Nonetheless, the latter could be caused by the overlap of the ol covering the anterior region of the il giving the impression of being smaller or lack of preservation.

An important remark regarding the anatomy of the jaw components reported in this work is that supposing that they preserved their original location and orientation (*i.e.*, an unlikely assumption as both usually change due to tissue degradation and other processes that cause displacement), the lower jaw has its major axis parallel to the apical-antapical axis of the whorl (Figs. 2–4, 10). This contrasts with occurrences in other specimens in which the lower jaw tends to be horizontal following the oral-apical axis parallel to the whorl (*e.g.*, Tanabe *et al.*, 2015a: fig. 10.6). The upper jaw is

long reaching the dorsum of the whorl, which constraints the possible vertical movements that both components (the upper and lower jaw) could perform. The interesting question is, how did this buccal apparatus function based on the shape of both jaws? A plausible solution would be a rotation following the longitudinal axis. The latter function could be tested experimentally using a virtual model of the jaw apparatus (Fig. 11). If we suppose the jaw apparatus components preserved their original orientation, the only possible movement is a rotation in the longitudinal plane. As follows, several pivot points located in the lower jaw can be tested to infer a viable performance. If the pivot point is near the dorsal area, the rotation does not allow the full aperture of the jaws, also generating an ineffective occlusion (Fig. 11.3). If the pivot point is around the ventral region of the lower jaw, the rostrum collides with the ol, hindering the aperture of the jaws (Fig. 11.4). Actually, due to the particular morphology and the size of the lower jaw, the position of the pivot point is very constrained. Based on the geometry of both jaws, it was found that the optimal position for the pivot point is in the ventral limit of the furrow in the lower jaw, interpreted here as a muscle attachment site (Fig. 11.5). Moreover, if the lower jaw is rotated to an almost horizontal position around this point, the r is positioned forward in a suitable orientation for feeding, resembling previous findings of ap as well (Fig. 11.6). In extant cephalopod species

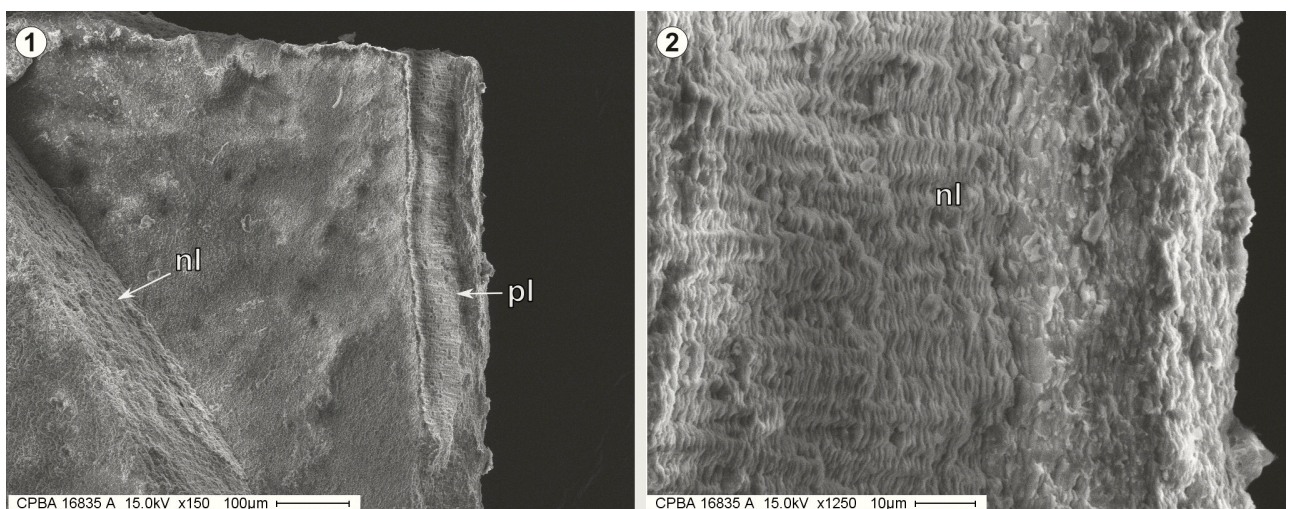
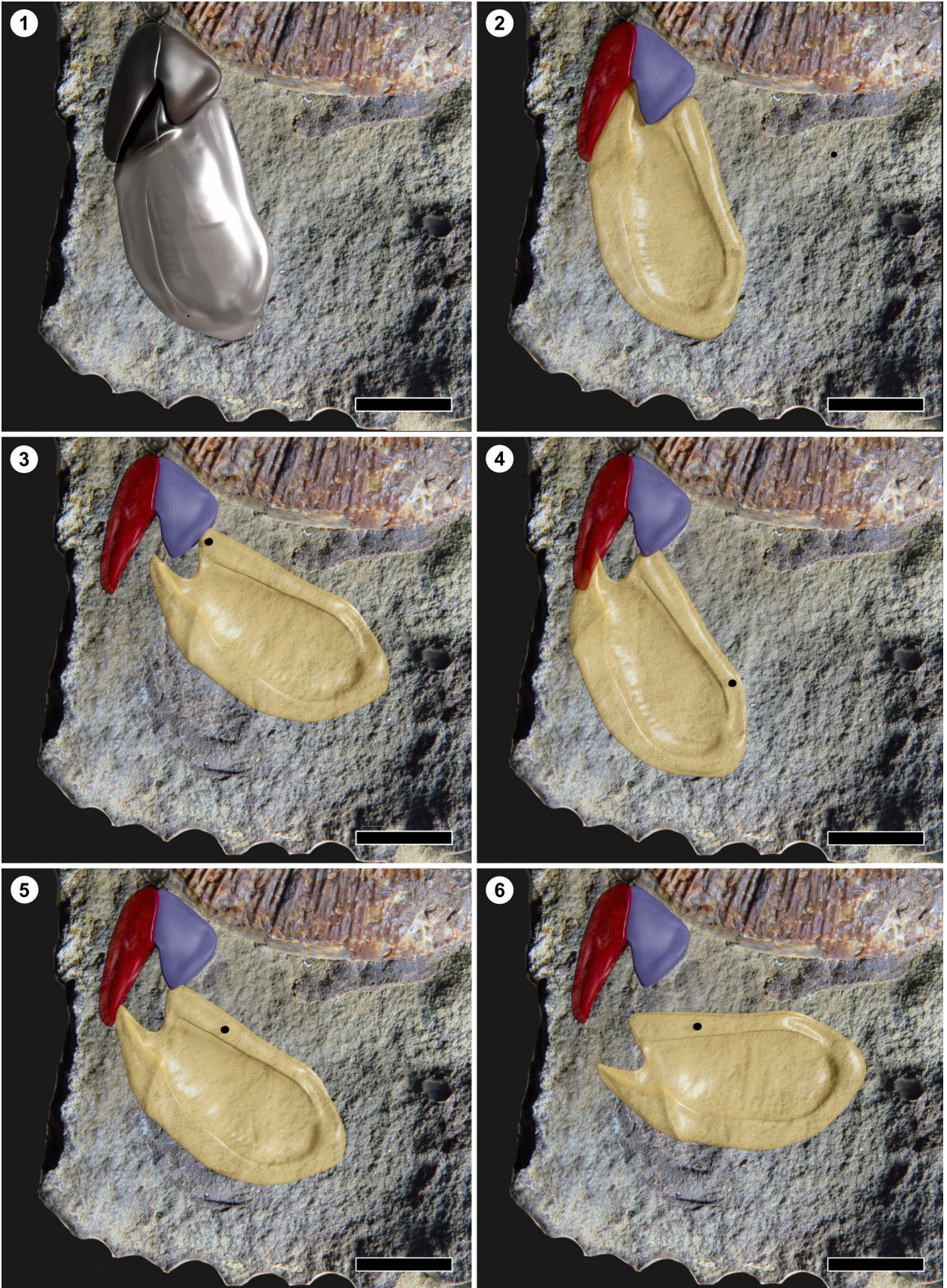


Figure 10. SEM images of a shell sample extracted from the *Maorites seymourianus*, CPBA-16835. 1, margin of the shell fragment showing the nacreous and prismatic layers. Note the columnar disposition of the carbonatic prisms; 2, close up of the nacreous layer showing the characteristic brick wall-like structure found in mollusks. This nacreous layer is composed of polygonal aragonite crystals that are 5–15 μm in diameter and separated by sheets of an interlamellar organic matrix (Nudelman *et al.*, 2008).



the lw of the upper and lower jaw do not articulate with each other. Instead, the upper and lower jaws (*i.e.*, ol) slide by each other, and the lw are embedded in muscular mass (see Tanabe *et al.*, 2015a: figs. 10.1, 10.3). The only points at which the jaws make contact are at the occlusion of the rostra and jaw angles (Uyeno & Kier, 2005). Further, in modern coleoids, jaw occlusion is principally executed by the upper jaw, associated with potent muscles attached to its lw (Uyeno & Kier, 2005). Hence, the upper jaw tends to be bigger than the lower jaw. An opposite pattern is observed in ammonoids, where the lower jaw is the largest component and its lw is more prominent in comparison. If these observations can be applied to ammonoids, then the position of the jaw components and the described functional morphology should be fairly accurate. Alternative possible jaw rotation movements performed either by the upper jaw or both jaws are presented in Supplementary material 3. For these simulations, the assumption that the structures preserved their original location and orientation is not fulfilled and the functionality is based uniquely on the geometry of both structures.

Regarding the enigmatic structures found in specimen CPBA-16835, a possibility is that some of them are just artefacts produced during the fossilization process or errors during the visualization of the RTI files. The latter can happen in the specular enhancement view due to the “face on mars effect”, in which specific shadows in digital imagery could lead to the misinterpretation of topographical features (Carlotto, 1988). This is conceivable, especially for the delicate traces found nearby the jaw apparatus. So, considering that at least some of these features correspond to remains of actual structures, we compared them to X-ray tomographic datasets from extant coleoids provided by Ziegler *et al.* (2018) and the anatomy of *Nautilus pompilius* (Linnaeus, 1758) described by Sasaki *et al.* (2010) to suggest possible interpretations.

The first structure interpreted was a smooth pr or elevation that seems to be attached to the posterior area of the lower jaw (Figs. 3–4). As mentioned previously, in extant cephalopods the buccal mass is principally articulated by a muscular system. These muscle fibres are tightly packed in a three-dimensional array forming a muscular hydrostat, firmly attached to the surrounding connective tissue and/or the buccal sheath (Uyeno & Kier, 2005; Tanabe, 2012; Tanabe *et al.*, 2012). Additionally, in *N. pompilius*, the jaws are tied with thick muscles connecting the inner surface of the lower jaw and the outer surface of the upper jaw (Sasaki *et al.*, 2010: fig. 5). It is unlikely that these soft tissues are preserved in the studied specimen. However, if these muscles were prominent and resistant enough, they might have left a mark on the fossil. Particularly, some features of the pr are consistent with this hypothesis, such as the prolongation towards the crest and the straight posterior margin, which may be signalling the attachment sites of a similar musculature to *N. pompilius*. Contrary, elements within the buccal cavity, such as the lateral buccal palps, salivary papilla, salivary glands, radula, and radular support system (Nixon & Young, 2003), would not have been preserved, at least in this section of the concretion.

The remaining structures, including the ds, the lo, and the organic fragment, are still under evaluation. However, XRD results indicate the presence of carbon and phosphorous suggesting the possible existence of organic remains in the ds. Complementary analyses (besides finding more complete specimens) will be required to identify these structures. The composition and origin of the organic translucent fragment are still uncertain and require further investigation (Fig. 7).

An oval mark on the phragmocone of the specimen CPBA-16835 (Fig. 9) is tentatively regarded as a lethal paleopathology, which may help to better understand the rare conditions which enabled this exceptional preservation.

Figure 11. Virtual models of the jaw apparatus of *Maorites seymourianus*, CPBA-16835, and inferred functional morphology assuming that the original position of the structures is preserved. **1**, reconstruction of chitinous jaws with mirrored complementary parts of the lower jaw (inferred complete structure); **2**, components of the jaw apparatus in their original position, in yellow the plate (lower jaw), in purple the inner lamella, and in red the outer lamella of the upper jaw; **3–6**, rotation of the lower jaw based on different pivot points (black circle). Note the jaw elements are large relative to the height of the whorl, restricting their possible movements; **3**, rotation with respect to a pivot point around the dorsal area; **4**, rotation relative to a pivot point around the ventral area; **5**, optimal position of the pivot point based on the morphology and geometry of the jaw components; **6**, same than 11.5 but the lower jaw was rotated horizontally parallel to the whorl. Scale bar= 10 mm.

Usually, shell perforations of the body chamber are not lethal for modern *Nautilus*, causing just a brief loss of buoyancy, and healing rapidly by the adjacent epithelium. The same is inferred for ammonoids (Keupp, 2012; Tsujino & Shigeta, 2012). However, in this case, the perforation was relatively large and long (around one-fifth of the whorl height) and encompassed at least two phragmocone chambers near the body chamber. Therefore, the functionality of the buoyancy apparatus might be more affected or completely lost as shown by Tsujino & Shigeta (2012). So, in a hypothetical scenario, the phragmocone was perforated and filled with seawater; in this state, the organism could not have retained its neutral buoyancy (Maeda & Seilacher, 1996; Tsujino & Shigeta, 2012; Wani & Gupta, 2015) and eventually succumbed (*i.e.*, by starvation, hypoxia, or thermal and/or osmotic shock). The ballasting would not have allowed postmortem transport enabling the retention of the structures observed on the specimen (Yacobucci, 2018). Burial after this event might have been rapid or under anoxic/euxinic conditions to preserve most of the observed structures (Parry *et al.*, 2018). Such conditions were possible due to the relatively high sedimentation rate estimated for the López de Bertodano Formation, around 4.7 cm/ky (Tobin *et al.*, 2012), and reported occurrences of intermittent euxinic conditions (Schoepfer *et al.*, 2017). Further, the large carbonate concretions, similar to where the fossil was found, are common in shallow marine sediments and can form early after burial preserving its original three-dimensional structure (Yoshida *et al.*, 2015). Carbonate concretions, contrary to sandstone concretions, tend to form small crystals and, under the right circumstances, can preserve even small details of the original organism, a process occasionally mediated by microbial mats and/or the decaying soft tissue (Marshall & Pirrie, 2013). An additional observation may have contributed to the discovery of the observed structures involving the presence of an ms layer (Fig. 4). The composition of the ms indicates the presence of chemically active fluids (probably from the nearby volcanic arc; Olivero, 2012). These active fluids percolated into the concretion, creating a weak point (*i.e.*, cleavage plain) in which it eventually naturally fractured.

The RTI technique used in this work allowed the recognition of the structures in CPBA-16835 during a regular re-

vision of the material, searching for alternative methods to replace ammonium chloride as a contrast agent given its toxic properties (*i.e.*, reported as a mucosal irritant; Feldmann, 1989; National Center for Biotechnology Information, 2022). Besides the enhanced visualization of surface features, this particular RTI technique can also be performed in the field, it does not require expensive surface scanning equipment, and the observations can be replicated relatively easily, making it valuable for research and teaching. RTI is particularly effective in depicting the ammonoid ornamentation, shell pathologies, and, in some cases, the sutural/septal elements, especially from the normal maps obtained from this process. Furthermore, the resolution of the resulting data largely depends on the camera specifications (*i.e.*, the number of megapixels). Some constraints of the method involve stable camera support to avoid movement during data acquisition, a reduced resolution due to the compression of the original images (and the space required for the black spheres), and minor considerations during data processing. There are also limitations related to the studied material. For example, in the studied specimen, the preservation of the previous whorl did not allow casting specific low light angles in the region of interest. However, despite these constraints, the RTI technique has the potential to become a standard complementary procedure in paleontological studies.

CONCLUSIONS

In this work, using a Reflectance Transformation Imaging (RTI) technique, we report the presence of the buccal apparatus and associated structures for a *Maorites seymourianus* specimen from the López de Bertodano Formation in Antarctica (Late Maastrichtian, latest Cretaceous). This is the first report of these components for the Kossmaticeratidae and the youngest report for ammonoids. Further, findings may encompass additional features, including evidence of possible muscular traces and other unidentified structures. We infer a sudden lethal event followed by rapid sedimentation in a shallow marine environment, based on a perforation found in the phragmocone. An ms in the body chamber would have prompted the cleavage plain allowing this special preservation. We concluded that the RTI technique used in this work is a practical and compelling technique for

paleontological studies, solving many of the limitations of similar methods based on the same principles presented before.

ACKNOWLEDGMENTS

Thanks to M. Tanús (Universidad de Buenos Aires, Buenos Aires, Argentina) for allowing studying the material under their care. Thanks to A. Concheyro (Universidad de Buenos Aires and Instituto Antártico Argentino, Buenos Aires, Argentina) for providing the specimen described in this study. Thanks to M. Pianetti (Instituto Nacional de Tecnología Industrial, Argentina) for their counselling and guidance using the SEM. Thanks to the researchers and technicians of the INQUIMAE-CONICET for allowing us to perform the DRX analysis in their facility. We are very grateful to C. Klug (Zurich University), who provided helpful feedback on this manuscript. Lastly, thanks to the critical suggestions of the anonymous reviewers and editors, who greatly improve the quality of this manuscript. This is the contribution R-441 of the Instituto de Estudios Andinos 'Don Pablo Groeber' (IDEAN, UBA-CONICET).

REFERENCES

- Barlow, L. A., Pittman, M., Butcher, A., Martill, D. M., & Kaye, T. G. (2021). Laser-stimulated fluorescence reveals unseen details in fossils from the Upper Jurassic Solnhofen Limestones. *Royal Society Open Science*, 8, 1–13. <https://doi.org/10.1098/rsos.211601>
- Béthoux, O., Llamosi, A., & Toussaint, S. (2016). Reinvestigation of *Protelytron permianum* (Insecta; Early Permian; USA) as an example for applying reflectance transformation imaging to insect imprint fossils. *Fossil Record*, 20(1), 1–7. <https://doi.org/10.5194/fr-20-1-2016>
- Blender Online Community (2022). Blender, a 3D Modelling and Rendering Package. <https://www.blender.org/download/releases/2-81/>
- Boute, R., Hupkes, M., Kollaard, N., Wouda, S., Seymour, K., & ten Wolde, L. (2018). Revisiting Reflectance Transformation Imaging (RTI): A Tool for Monitoring and Evaluating Conservation Treatments. *IOP Conference Series: Materials Science and Engineering*, 364, 012060. <https://doi.org/10.1088/1757-899x/364/1/012060>
- Carlotto, M. (1988). Digital imagery analysis of unusual Martian surface features. *Applied optics*, 27, 1926–33. <https://doi.org/10.1364/AO.27.001926>
- Cherns, L., Spencer, A. R. T., Rahman, I. A., Garwood, R. J., Reedman, C., Burca, G., Turner, M. J., Hollingworth, N. T. J., & Hilton, J. (2021). Correlative tomography of an exceptionally preserved Jurassic ammonite implies hyponome-propelled swimming. *Geology*, 50, 397–401. <https://doi.org/10.1130/G49551.1>
- Cunningham, J. A., Rahman, I. A., Lautenschlager, S., Rayfield, E. J., & Donoghue, P. C. J. (2014). A virtual world of paleontology. *Trends in Ecology & Evolution*, 29(6), 347–357. <https://doi.org/10.1016/j.tree.2014.04.004>
- Degen, T., Sadki, M., Bron, E., König, U., & Nénert, G. (2014). The High-Score suite. *Powder Diffraction*, 29(S2), S13–S18. <https://doi.org/10.1017/S0885715614000840>
- Feldmann, R. (1989). Whitening fossils for photographic purposes. *The Paleontological Society Special Publications*, 4, 342–346. <https://doi.org/10.1017/S2475262200005323>
- Giovannetti, G., Guerrini, A., & Salvadori, P. A. (2016). Magnetic resonance spectroscopy and imaging for the study of fossils. *Magnetic Resonance Imaging*, 34(6), 730–742. <https://doi.org/10.1016/j.mri.2016.03.010>
- Guo, J., Parry, L. A., Vinther, J., Edgecombe, G. D., Wei, F., Zhao, J., Zhao, Y., Béthoux, O., Lei, X., Chen, A., Hou, X., Chen, T., & Cong, P. (2022). A Cambrian tommotiid preserving soft tissues reveals the metamerism ancestry of lophophorates. *Current Biology*, 32(21), 4769–4778.e2. <https://doi.org/10.1016/j.cub.2022.09.011>
- Hammer, Ø., & Spocova, J. (2013). Virtual whitening of fossils using polynomial texture mapping. *Palaeontologia Electronica*, 16.2.4T. <https://doi.org/10.26879/384>
- Hammer, Ø., Bengtson, S., Malzbender, T., & Gelb, D. (2002). Imaging fossils using reflectance transformation and interactive manipulation of virtual light sources. *Palaeontologia Electronica*, 5(4), 1–9.
- Hoffmann, R., Schultz, J. A., Schellhorn, R., Rybacki, E., Keupp, H., Gerden, S. R., Lemanis, R., & Zachow, S. (2013). Non-invasive imaging methods applied to neo- and paleo-ontological cephalopod research. *Biogeosciences Discuss*, 11(10), 2721–2739. <https://doi.org/10.5194/bg-11-2721-2014>
- Keupp, H. (2012). Atlas zur Paläopathologie der Cephalopoden. *Berliner paläobiologische Abhandlungen*, 12, 1–390.
- Kilian, W., & Reboul, P. (1909). Les Cephalopodes neocretacées des Iles Seymour et Snow ill. *Wissenschaftliche Ergebnisse der Schwedischen Südpolar-Expedition 1901-1903, Stockholm*, 3, 1–75.
- Klug, C., & Hoffmann, R. (2015). Ammonoid Septa and Sutures. In C. Klug, D. Korn, K. De Baets, I. Kruta, & Mapes (Eds.), *Ammonoid Paleobiology: From anatomy to ecology. Topics in Geobiology, vol 43* (pp. 45–90). Springer. https://doi.org/10.1007/978-94-017-9630-9_3
- Klug, C., & Lehmann, J. (2015). Soft Part Anatomy of Ammonoids: Reconstructing the Animal Based on Exceptionally Preserved Specimens and Actualistic Comparisons In C. Klug, D. Korn, K. De Baets, I. Kruta, & R. H. Mapes (Eds.), *Ammonoid Paleobiology: From anatomy to ecology. Topics in Geobiology, vol 43* (pp. 507–529). Springer. https://doi.org/10.1007/978-94-017-9630-9_12
- Klug, C., Korn, D., Landman, N. H., Tanabe, K., De Baets, K., & Nagliik, C. (2015). Describing Ammonoid Conchs. In C. Klug, D. Korn, K. De Baets, I. Kruta, & R. H. Mapes (Eds.), *Ammonoid Paleobiology: From anatomy to ecology. Topics in Geobiology, vol 43* (pp. 3–24). Springer. https://doi.org/10.1007/978-94-017-9630-9_1
- Klug, C., Landman, N. H., Fuchs, D., Mapes, R. H., Pohle, A., Guériau, P., Reguer, S., & Hoffmann, R. (2019). Anatomy and evolution of the first Coleoidea in the Carboniferous. *Communications Biology*, 2, 280. <https://doi.org/10.1038/s42003-019-0523-2>
- Kozub, D., Shapoval, J., Yatsenko, S., Starikh, V., & Dobarskyi, A. (2022). *Helicon Focus 8.0.4. Helicon Soft Ltd*. <https://www.heliconsoft.com/heliconsoft-products/helicon-focus/>
- Kröger, B., Vinther, J., & Fuchs, D. (2011). Cephalopod origin and evolution: A congruent picture emerging from fossils, development and molecules: Extant cephalopods are younger than previously realised and were under major selection to become agile, shell-less predators. *Bioessays*, 33(8), 602–613. <https://doi.org/10.1002/bies.201100001>
- Kruta, I., Bardin, J., Smith, C. P. A., Tafforeau, P., & Landman, N. H. (2020). Enigmatic hook-like structures in Cretaceous ammonites (Scaphitidae). *Palaeontology*, 63, 301–312. <https://doi.org/10.1111/pala.12457>
- Landman, N., Goolaerts, S., Jagt, J., Jagt-Yazykova, E., & Machalski, M. (2015). Ammonites on the Brink of Extinction: Diversity, Abundance, and Ecology of the Order Ammonoidea at the Cretaceous/Paleogene (K/Pg) Boundary Comparisons In C. Klug, D.

- Korn, K. De Baets, I. Kruta, & R. Mapes (Eds.), *Ammonoid Paleobiology: From anatomy to ecology. Topics in Geobiology, vol 43* (pp. 497–553). Springer. https://doi.org/10.1007/978-94-017-9633-0_19
- Linnaeus, C. v. (1758). *Systema Naturae: per regna tria naturæ, secundum classes, ordines, genera, species, cum characteribus, differentiis, synonymis, locis, vol. 1. Laurentii Salvii*, Stockholm.
- Macellari, C. (1986). Late Campanian–Maastrichtian Ammonite Fauna from Seymour Island (Antarctic Peninsula). *Journal of Paleontology*, *60*, 1–55. <https://doi.org/10.1017/S0022336000060765>
- Macellari, C. (1988). Stratigraphy, sedimentology, and paleoecology of Upper Cretaceous/Paleocene shelf-deltaic sediments of Seymour Island. In R. M. Feldmann, & Woodburne (Eds.), *Geology and Paleontology of Seymour Island Antarctic Peninsula* (pp. 25–53). Geological Society of America. <https://doi.org/10.1130/MEM169-p25>
- Maeda, H., & Seilacher, A. (1996). Ammonoid Taphonomy. In N. H. Landman, K. Tanabe, & R. A. Davis (Eds.), *Ammonoid Paleobiology. Topic in Geobiology, vol 13* (pp. 543–578). Springer. https://doi.org/10.1007/978-1-4757-9153-2_14
- Marshall, J. D., & Pirrie, D. (2013). Carbonate concretions—explained. *Geology Today*, *29*(2), 53–62. <https://doi.org/10.1111/gto.12002>
- Microsoft-Corporation (2015). *Image Composite Editor 2.0.3.0. Microsoft Research ICE*. <https://www.microsoft.com/en-us/research/product/computational-photography-applications/image-composite-editor/>
- Min, J., Jeong, S., Park, K., Choi, Y., Lee, D., Ahn, J., Har, D., & Ahn, S. (2021). Reflectance transformation imaging for documenting changes through treatment of Joseon dynasty coins. *Heritage Science*, *9*(1), 105–116. <https://doi.org/10.1186/s40494-021-00584-3>
- Mironenko, A. A., & Mitta, V. V. (2023). The first record of jaws of Boreal Valanginian ammonites (Cephalopoda, Polyptychitidae). *Cretaceous Research*, *142*, 105370. <https://doi.org/10.1016/j.cretres.2022.105370>
- Montes, M., Beamud, E., Nozal, F., & Santillana, S. (2019). Late Maastrichtian–Paleocene chronostratigraphy from Seymour Island, James Ross Basin, Antarctic Peninsula: Eustatic controls on sedimentation. *Advances in Polar Science*, *30*, 303–327. <https://doi.org/10.13679/j.advps.2018.0045>
- Morita, M. M., Novoa, F. D., & Bilmes, G. M. (2019). Reflectance transformation imaging. First applications in cultural heritage in Argentina. *Journal of Archaeological Science: Reports*, *26*, 101899. <https://doi.org/10.1016/j.jasrep.2019.101899>
- Morón-Alfonso, D. (2019). Exploring the paleobiology of ammonoids (Cretaceous, Antarctica) using non-invasive imaging methods. *Palaeontologia Electronica*, *22.3.57*, 1–17. <https://doi.org/10.26879/1007>
- National Center for Biotechnology Information. (2022). *PubChem Compound Summary for CID 25517, Ammonium Chloride*. National Center for Biotechnology Information. <https://pubchem.ncbi.nlm.nih.gov/compound/Ammonium-Chloride>
- Nixon, M. & Young, J. Z. (2003). *The brains and lives of cephalopods, vol. 1*. Oxford University Press.
- Nudelman, F., Shimoni, E., Klein, E., Rousseau, M., Bourrat, X., Lopez, E., Addadi, L., & Weiner, S. (2008). Forming nacreous layer of the shells of the bivalves *Atrina rigida* and *Pinctada margaritifera*: An environmental- and cryo-scanning electron microscopy study. *Journal of Structural Biology*, *162*, 290–300. <https://doi.org/10.1016/j.jsb.2008.01.008>
- Olivero, E. (2012). Sedimentary cycles, ammonite diversity and palaeoenvironmental changes in the Upper Cretaceous Marambio Group, Antarctica. *Cretaceous Research*, *34*, 348–366. <https://doi.org/10.1016/j.cretres.2011.11.015>
- Palma, G., Corsini, M., Cignoni, P., Scopigno, R., & Mudge, M. (2010). Dynamic shading enhancement for reflectance transformation imaging. *Journal on Computing and Cultural Heritage*, *3*(2), 1–20. <https://doi.org/10.1145/1841317.1841321>
- Pan, Y., Hu, L., & Zhao, T. (2019). Applications of chemical imaging techniques in paleontology. *National Science Review*, *6*, 1–14. <https://doi.org/10.1093/nsr/nwy107>
- Parry, L. A., Smithwick, F., Nordén, K. K., Saitta, E. T., Lozano-Fernandez, J., Tanner, A. R., Caron, J. -B., Edgecombe, G. D., Briggs, D. E. G., & Vinther, J. (2018). Soft-bodied fossils are not simply rotten carcasses – toward a holistic understanding of exceptional fossil preservation. *Bioessays*, *40*(1), 1700167. <https://doi.org/10.1002/bies.201700167>
- Pérez-Ramos, A., & Figueirido, B. (2020). Toward an “ancient” virtual world: improvement methods on X-ray CT data processing and virtual reconstruction of fossil skulls. *Frontiers in Earth Science*, *8*, 1–23. <https://doi.org/10.3389/feart.2020.00345>
- Peterman, D., Mikami, T., & Inoue, S. (2020). The balancing act of *Nipponites mirabilis* (Nostoceratidae, Ammonoidea): Managing hydrostatics throughout a complex ontogeny. *PLOS ONE*, *15*(8), e0235180. <https://doi.org/10.1371/journal.pone.0235180>
- Peterman, D., Ciampaglio, C., Shell, R., & Yacobucci, M. (2019). Mode of life and hydrostatic stability of orthoconic ectocochleate cephalopods: Hydrodynamic analyses of restoring moments from 3D printed, neutrally buoyant models. *Acta Palaeontologica Polonica*, *64*, 441–460. <https://doi.org/10.4202/app.00595.2019>
- Sasaki, T., Shigeno, S., & Tanabe, K. (2010). Anatomy of living *Nautilus*: Reevaluation of primitiveness and comparison with Coleoidea. In K. Tanabe, Y. Shigeta, T. Sasaki, & H. Hirano (Eds.), *Cephalopods - Present and Past* (pp. 35–66). Tokai University Press.
- Scasso, R. A., Prámparo, M. B., Vellekoop, J., Franzosi, C., Castro, L. N., & Sinninghe Damsté, J. S. (2020). A high-resolution record of environmental changes from a Cretaceous–Paleogene section of Seymour Island, Antarctica. *Palaeogeography, Palaeoclimatology, Palaeoecology*, *555*, 109844. <https://doi.org/10.1016/j.palaeo.2020.109844>
- Schoepfer, S. D., Tobin, T. S., Witts, J. D., & Newton, R. J. (2017). Intermittent euxinia in the high-latitude James Ross Basin during the latest Cretaceous and earliest Paleocene. *Palaeogeography, Palaeoclimatology, Palaeoecology*, *477*, 40–54. <https://doi.org/10.1016/j.palaeo.2017.04.013>
- Schroer, C. (2012). Advanced imaging tools for museum and library conservation and research. *Bulletin of the American Society for Information Science and Technology*, *38*, 38–42. <https://doi.org/10.1002/bult.2012.1720380310>
- Smith, C. P. A., Landman, N. H., Bardin, J., & Kruta, I. (2021). New evidence from exceptionally “well-preserved” specimens sheds light on the structure of the ammonite brachial crown. *Scientific Reports*, *11*, 11862. <https://doi.org/10.1038/s41598-021-89998-4>
- Sutton, M., Rahman, I., & Garwood, R. (2016). Virtual Paleontology: An Overview. *The Paleontological Society Papers*, *22*, 1–20. <https://doi.org/10.1017/scs.2017.5>
- Tajika, A., Naglik, C., Morimoto, N., Pascual-Cebrian, E., Hennhöfer, D., & Klug, C. (2015). Empirical 3D model of the conch of the Middle Jurassic ammonite microconch *Normannites*: its buoyancy, the physical effects of its mature modifications and speculations on their function. *Historical Biology*, *27*, 181–191. <https://doi.org/10.1080/08912963.2013.872097>
- Takeda, Y., Tanabe, K., Sasaki, T., Uesugi, K., & Hoshino, M. (2016).

- Non-destructive analysis of in situ ammonoid jaws by synchrotron radiation X-ray micro-computed tomography. *Palaeontologia Electronica*, 19, 1–13. <https://doi.org/10.26879/697>
- Tanabe, K. (2012). Comparative morphology of modern and fossil coleoid jaw apparatuses. *Neues Jahrbuch für Geologie und Paläontologie - Abhandlungen*, 266, 9–18. <https://doi.org/10.1127/0077-7749/2012/0243>
- Tanabe, K., Landman, N. H., & Kruta, I. (2012). Microstructure and mineralogy of the outer calcareous layer in the lower jaws of Cretaceous Tetragnotoidea and Desmoceratoidea (Ammonoidea). *Lethaia*, 45(2), 191–199. <https://doi.org/10.1111/j.1502-3931.2011.00272.x>
- Tanabe, K., Kruta, I., & Landman, N. H. (2015a). Ammonoid buccal mass and jaw apparatus. In C. Klug, D. Korn, K. De Baets, I. Kruta, & Mapes, (Eds.), *Ammonoid Paleobiology: From anatomy to ecology. Topics in Geobiology*, vol. 43 (pp. 429–484). Springer. https://doi.org/10.1007/978-94-017-9630-9_10
- Tanabe, K., Sasaki, T., & Mapes, R. H. (2015b). Soft-Part Anatomy of the Siphuncle in Ammonoids. In C. Klug, D. Korn, K. De Baets, I. Kruta, & R. H. Mapes (Eds.), *Ammonoid Paleobiology: From anatomy to ecology. Topics in Geobiology*, vol. 43 (pp. 531–544). Springer. https://doi.org/10.1007/978-94-017-9630-9_13
- Tanabe, K., Aiba, D., & Abe, J. (2021). The jaw apparatus of the Late Cretaceous heteromorph ammonoid *Turrilites costatus* from central Hokkaido, Japan. *Bulletin of the Mikasa City Museum*, 24, 1–8.
- Tobin, T. S., Ward, P. D., Steig, E. J., Olivero, E. B., Hilburn, I. A., Mitchell, R. N., Diamond, M. R., Raub, T. D., & Kirschvink, J. L. (2012). Extinction patterns, $\delta^{18}\text{O}$ trends, and magnetostratigraphy from a southern high-latitude Cretaceous–Paleogene section: Links with Deccan volcanism. *Palaeogeography, Palaeoclimatology, Palaeoecology*, 350–352, 180–188. <https://doi.org/10.1016/j.palaeo.2012.06.029>
- Tsujino, Y. & Shigeta, Y. (2012). Biological response to experimental damage of the phragmocone and siphuncle in *Nautilus pompilius* Linnaeus. *Lethaia*, 45, 443–449. <https://doi.org/10.1111/j.1502-3931.2012.00306.x>
- Uyeno, T. & Kier, W. (2005). Functional morphology of the cephalopod buccal mass: A novel joint type. *Journal of Morphology*, 264, 211–222. <https://doi.org/10.1002/jmor.10330>
- Van Bocxlaer, B. & Schultheiß, R. (2010). Comparison of morphometric techniques for shapes with few homologous landmarks based on machine-learning approaches to biological discrimination. *Paleobiology*, 36, 497–515.
- Wani, R. & Gupta, N. S. (2015). Ammonoid Taphonomy. In C. Klug, D. Korn, K. De Baets, I. Kruta, & R. H. Mapes (Eds.), *Ammonoid Paleobiology: From macroevolution to paleogeography. Topics in Geobiology*, vol 43 (pp. 555–598). Springer Netherlands. https://doi.org/10.1007/978-94-017-9633-0_20
- Witts, J. D., Bowman, V. C., Wignall, P. B., Alistair Crame, J., Francis, J. E., & Newton, R. J. (2015). Evolution and extinction of Maastrichtian (Late Cretaceous) cephalopods from the López de Bertodano Formation, Seymour Island, Antarctica. *Palaeogeography, Palaeoclimatology, Palaeoecology*, 418, 193–212. <https://doi.org/10.1016/j.palaeo.2014.11.002>
- Yacobucci, M. M. (2018). Postmortem transport in fossil and modern shelled cephalopods. *PeerJ*, 6, e5909–e5909. <https://doi.org/10.7717/peerj.5909>
- Yoshida, H., Ujihara, A., Minami, M., Asahara, Y., Katsuta, N., Yamamoto, K., Sirono, S. -i., Maruyama, I., Nishimoto, S., & Metcalfe, R. (2015). Early postmortem formation of carbonate concretions around tusk-shells over week-month timescales. *Scientific Reports*, 5, 14123. <https://doi.org/10.1038/srep14123>
- Ziegler, A., Bock, C., Ketten, D., Mair, R., Mueller, S., Nagelmann, N., Pracht, E., & Schröder, L. (2018). Digital three-dimensional imaging techniques provide new analytical pathways for malacological research. *American Malacological Bulletin*, 36, 248–273. <https://doi.org/10.4003/006.036.0205>

doi: 10.5710/PEAPA.28.12.2022.430

Recibido: 9 de junio 2022

Aceptado: 28 de diciembre 2022

Publicado: 1 de marzo 2023



This work is licensed under

CC BY-NC 4.0

